Final Technical Report

ICME Guided Development of Advanced Cast Aluminum Alloys for Automotive Engine Applications (ADAPA)

Award Number: DE-EE0006020

Recipient: Ford Motor Company

Working Partners: Alcoa, University of Michigan, MAGMA Foundry Technologies, Inc.

Report Period: March 1 , 2013 to August 31, 2018

Date of Report: Nov 30, 2018

1. **Recipient:** Ford Motor Company
   Award Number: DE-EE0006020

   Working Partners: Ford Motor Company, Alcoa, University of Michigan, MAGMA Foundry Technologies, Inc.
   Cost-Sharing Partners: Ford Motor Company, Alcoa, MAGMA Foundry Technologies, Inc.

   Principle Investigator: Mei Li, (313) 206-4219, mli9@ford.com
   Ford Contracts Manager: Melissa Hendra, (313) 594-4714, mhendra@ford.com

   DOE Program Manager: John R. Terneus, (304) 285-4254, John.Turneus@netl.doe.gov
   DOE Contract Manager: Amanda Lopez, (304) 285-5223, Amanda.Lopez@netl.doe.gov
   DOE Tech. Dev. Manager: Jerry Gibbs, 202-586-1182, Jerry.Gibbs@ee.doe.gov

2. **Project Title:** ICME Guided Development of Advanced Cast Aluminum Alloys for Automotive Engine Applications (ADAPA)

3. **Report Period:** July 1, 2018 to August 31, 2018
   Date of Report: Nov, 31, 2018

4. **Project Objectives:**
   - To develop a new class of advanced, cost competitive aluminum casting alloys providing a 25% improvement in component strength relative to components made with A319 or A356 alloys using sand and semi-permanent casting processes for high-performance engine applications.
   - To demonstrate the power of Integrated Computational Materials Engineering (ICME) tools for accelerating the development of new materials and processing techniques, as well as to identify the gaps in ICME capabilities.
   - To develop comprehensive cost models to ensure that components manufactured with these new alloys do not exceed 110% of the cost using incumbent alloys A319 or A356.
   - To develop a technology transfer and commercialization plan for deployment of these new alloys in automotive engine applications.
   - The key targets and baseline are shown in the table below.

5. Background:

Recently legislated fuel economy standards require new U.S. passenger vehicles to achieve at least 34.1 MPG on average by model year 2016 and 58 MPG by 2030, up from 28.8 MPG today. Two major methods of achieving improved fuel economy in passenger vehicles are reducing the weight of the vehicle and developing high-performance engines. To increase engine efficiency, however, the maximum operation temperature of these components has increased from approximately 170°C in earlier engines to peak temperatures well above 200°C in recent engines. The increase in the operational temperatures requires a material with optimized properties in terms of tensile, creep and fatigue strength. This program focusses on developing advanced cast aluminum alloys for automotive engine applications to meet these challenging requirements.

6. Milestone Review:

Major milestones are shown in the following table:

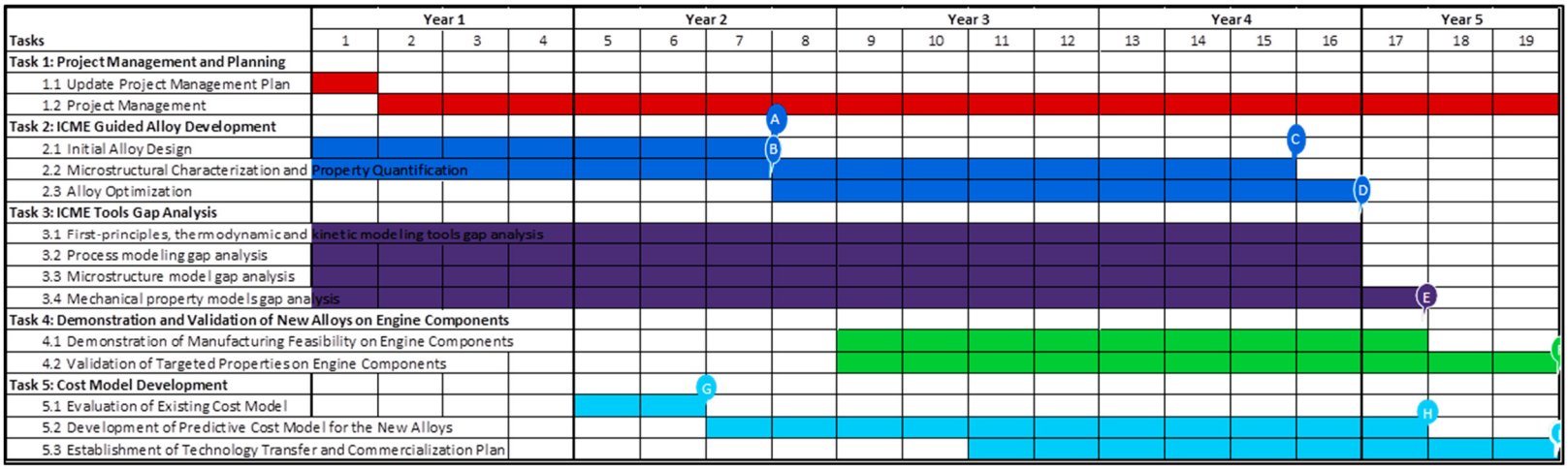

A	Complete the initial alloy design
B	Complete Microstructural Characterization and Property Quantification for initial alloy design
C	Complete Microstructural Characterization and Property Quantification for optimized alloys
D	Complete the optimization of new alloys to meet or exceed the desired targets
E	Complete ICME Tools Gap Analysis
F	Complete the demonstration and Validation of New Alloys on Engine Components
G	Complete the evaluation of Existing Cost Model and establish the new cost model development plan
H	Complete the new cost model development
I	Deliver the Technology Transfer and Commercialization Plan

A detailed milestones list, the milestone description and the status are shown in the following table:

Milestone ID Number	Milestone Description	Original Milestone Date	Status	New/Revised Milestone Date
1.1 Update Project Management Plan (PMP)	Negotiate subcontract with University of Michigan	04/15/2013	Completed	
	Negotiate subcontract with MAGMA Foundry Technologies Inc.	04/15/2013	Completed	
	Negotiate subcontract with Alcoa	08/15/2013	Completed	
1.2 Project Management	Lay out the program strategy and have consensus on deliverables	02/15/2013	Completed	
	Agreement on the new alloy requirements and testing protocol	03/15/2013	Completed	
2.1 Initial Alloy Design	Literature survey	05/30/2013	Completed	
	Initial alloy compositions determined and cast	10/30/2013	Completed	
2.2 Microstructural Characterization and Property Qualification	Characterize the microstructure and property of the initial alloys and strategy for improvement	11/30/2014	Completed	
2.3 Alloy Optimization	Optimum alloy compositions are determined and cast	11/30/2015	Completed	

	Characterize the microstructure and property of the optimum alloys to confirm the targets are met	11/30/2015	Completed	
3.1 Thermodynamic and Kinetic Modeling	Thermodynamic and kinetic modeling of the initial alloys	11/30/2014	Completed	
	Thermodynamic and kinetic modeling of the optimized alloys	11/30/2015	Completed	
	Identify the ICME gaps in thermodynamic and kinetic Modeling	11/30/2015	Completed	
3.2 Process Modeling and Gap Analysis	Process modeling of the initial test mold casting	11/30/2014	Completed	
	Process modeling of the prototyping casting	11/30/2015	Completed	
	Identify the ICME gaps in casting process modeling	11/30/2015	Completed	
3.3 Microstructure Modeling and Gap Analysis	Microstructure model and compare with experimental characterization	05/30/2015	Completed	
	Identify the ICME gaps in casting and heat treatment microstructure modeling	11/30/2015	Completed	
3.4 Mechanical Property Modeling and Gap Analysis	Mechanical property model and compare with experimental characterization	05/30/2015	Completed	

	Identify the ICME gaps in casting and heat treatment microstructure modeling	11/30/2015	Completed	
4.1 Demonstration on Engine Components	Demonstration of Manufacturing Feasibility on Engine Components	11/30/2015	Completed	
4.2 Validation on Engine Components	Validation of Targeted Properties on Engine Components	11/30/2015	Completed	
5.1 Evaluation of Existing Cost Model	Evaluate an existing cost model developed for Low Pressure Sand Casting (LPSC) and develop plan to support the current project	11/30/2014	Completed	
5.2 Development of Predictive Cost Model for the New Alloys	Develop comprehensive cost models inclusive of the costs of alloy production, casting and heat treatment processing and finishing	11/30/2015	Completed	
5.3 Technology Transfer	Establishment of Technology Transfer & Commercialization plan	01/30/2016	Completed	

7. Results and Discussion

Task 1: Alloy Design and Mechanical Properties

In the past five years, more than 50 different combinations of alloys and heat-treatment were proposed and more than 1000 specimens were characterized included tensile and

fatigue testing at room and elevated temperatures. Two combinations exhibit superior elevated temperature performance and can meet all the requirements proposed by DOE. The alloy is 319-type alloy with addition of transition metal (TM) elements that has been approved to benefit elevated temperatures performance. With different casting methods and heat treatments, this alloy is applicable for cylinder heads and engine blocks. For cylinder head applications, Ford-SPMC-3Stage is prepared by semi-permanent mold and utilizes a three-stage heat treatment, designed to maximize the room-temperature properties, like yield strength and ductility, while maintaining the effects of TM additions for improvement of the endurance limit at 150 ˚C. For engine block applications, Ford-HPDC-T5 is utilized with the high-pressure die casting process, and with a T5 heat treatment, which shows a significant improvement to the endurance limit at 180 ˚C.

Ford-SPMC and Ford-HPDC, and two benchmark alloys, AA319 that is the baseline alloy and AS7GU that is currently used alloy for high performance automotive engine, were cast into torpedo shape. Heat treatment for these torpedo samples were performed in a fan-assisted resistance furnace, followed by quench into water. The quasi-static tensile test results of these alloys from room temperature to 300 °C are summarized in figure 1. First of all, as figure 7.1.1a shown, 300 °C YS of tested alloys exhibits a significant decrease after 100 hour pre-exposure at this temperature. It's obvious that YS of AA319-T7 after pre-exposure cannot meet DOE requirement, while YS of Ford-SPMC with both T7 and three-stage heat treatment are above the target. Since the alloys used in automotive engines are always exposed to hot environment (above 150 °C) for very long time, the samples for elevated temperature test need to be pre-exposed at testing temperatures for 100 hour to ensure the obtained results are closed to those from the real engine components. Second, figure 1b and d indicate that both YS and UTS of test alloys decrease with increasing of temperatures. The decreasing of Ford-HPDC-T5, however, is much slower than the other alloys. Although Ford-HPDC-T5 has the lowest YS and UTS at room temperature, which is due to the lack of solution treatment in T5 heat treatment, its YS and UTS are higher than the other alloys once the testing temperatures are above 250 °C. At 300 °C, YS and UTS of Ford-HPDC-T5 exhibits a 30% increasement, comparing with other alloys. Based on our experimental data, YS and UTS of Ford-HPDC-T5 are more than twice as high as that of currently used engine block alloy, ADC12Z, with T5 heat treatment condition from room temperature to 300 °C. It's well known that the strengthening precipitates of AA319 alloys are mainly Θ'-Al_2Cu forming during artificial aging and they coarsen very rapidly when they are exposed to 300 °C.

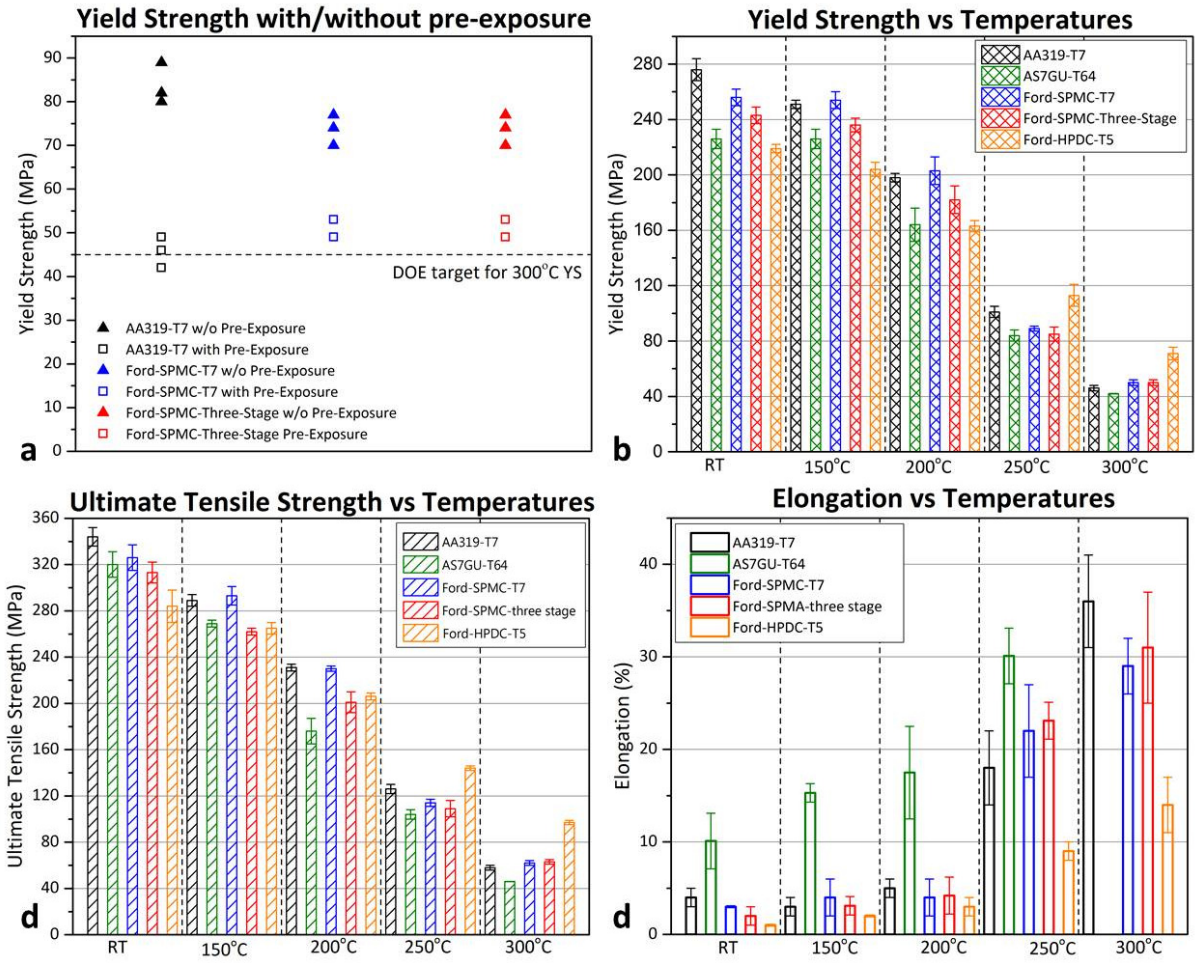

Figure 7.1.1: Graphical representation of quasi-static tensile test results of AA319-T7, AS7GU-T64, Ford-SPMC-T7, and Ford-SPMC-Three-Stage, and Ford-HPDC-T5 from room temperature to 300°C

According to figure 7.1.1, it's indicated that the improvement of both YS and UTS of Ford-SPMC with T7 and novel three-stage heat treatment is very limit, comparing to their baseline alloy, AA319. In fact, although YS of AA319-T7 is hard to meet the DOE requirement at 300 °C, its YS and UTS are higher than that of Ford-SPMC at low temperatures. In the most situations, however, the failure of automotive cylinder head is dominated by fatigue rather than tensile. As a result, the high cycle fatigue (HCF) strength is a more important mechanical parameter than YS and UTS for cylinder head alloys, especially, at elevated temperatures (>120 °C). The HCF tests were performed on a servo-hydraulic testing machine at 70 Hz. The stress ratio for all HCF tests is -1 and the criterion for HCF life is final fracture of the sample. The HCF data are processed by Random Fatigue Limit (RFL) model and HCF strength predicted by this model is summarized in table 7.2.1.

Firstly, although no improvement is observed in room temperature HCF strength, Ford-SPMC-three-stage has much higher 120 °C HCF strength than AA319-T7 and Ford-SPMC-T7. This result indicates that elevated temperature HCF strength benefits from novel additions only through the designed heat treatment. No enhancement is achieved through the chemistry solely, since AA319-T7 and Ford-SPMC-T7 have comparable HCF strength at 120 °C. Secondly, the enhanced HCF fatigue of Ford-SPMC-three-stage is maintained at least to 180 °C. Thus, Ford-SPMC-three-stage has better elevated temperature HCF strength than AS7GU-T64, the currently used alloy for high perforance cylinder head, because HCF strength of AS7GU drops from 83±11 MPa at 120 °C to 62±6 MPa at 150 °C. Thirdly, Ford-HPDC-T5 also has very excellent HCF strength at elevated temperatures. To the knowledge of the authors, Ford-SPMC-three-stage and Ford-HPDC-T5 have the best HCF performance at elevated temperatures (>150 °C) in all the aluminum alloys intend for engine application.

Table 7.1.1 Endurance limit of test alloys at different temperatures calculated by RFL model

	RT	120 °C	150 °C	180 °C	200 °C
AA319-T7	88±6 MPa	64±6 MPa	< 64 MPa	<<64 MPa	
AS7GU-T64	89±6 MPa	83±11 MPa	62±6 MPa	<62 MPa	
Ford-SPMC-T7	N/A	68±17 MPa	<68 MPa	<<68 MPa	
Ford-SPMC-3Stage	N/A	91±12 MPa	91±12 MPa	92±12 MPa	
Ford-HPDC-T5	N/A	N/A	97±7 MPa	98±9 MPa	85±2 MPa

Task 2: Microstructure Characterization

The microstructures of Ford-SPMC and Ford-HPDC at different heat treatment stages were characterized using advanced electron microscope, including scanning electron microscope (SEM), transmission electron microscope (TEM), electron probe micro-analysis (EMPA), and atom probe tomography (APT).

Firstly, TM elements in Ford-SPMC after solidification were found to form plate shape primary phases and dissolve in Al-matrix. Two types of TM-containing primary phases with different contrasts in back scatter electron (BSE) mode were found (Figure 7.2.1 (a)-(d)) showing the plate phase with grey contrast (Type I) and the phase with bright contrast (Type II), respectively. Furthermore, energy-dispersive X-ray spectroscopy (EDS) mapping scan was conducted in this area. EDS results indicated that more V and Ti concentrated in Type I phase and Type II phase was enriched in Zr and traces of V and Ti. Analysis using TEM was performed to clarify the phase type of Zr-containing primary phases. The crystal structure of Type I primary phase was identified as D022 by selected area electron diffraction (SAED). The bright field TEM image (Figure 7.2.2(a)) and corresponding SAED

patterns from different zone axis of Type I phase (Figure 7.2.2(c)~(e)) determined its crystal structure to be Do22 type, as illustrated in Figure 7(b). On the other hand, Type II was determined as Do23, as shown from Figure 7.2.2(f)-(g). In addition, the microsegregation profile of alloying element Zr versus solidification fraction was quantitatively characterized using the EPMA, as shown in Figure 7.2.3. The concentration of Zr decreases with increasing the solid fraction, indicating that Zr segregates into the dendrite core, which is typical microsegregation behavior of peritectic.

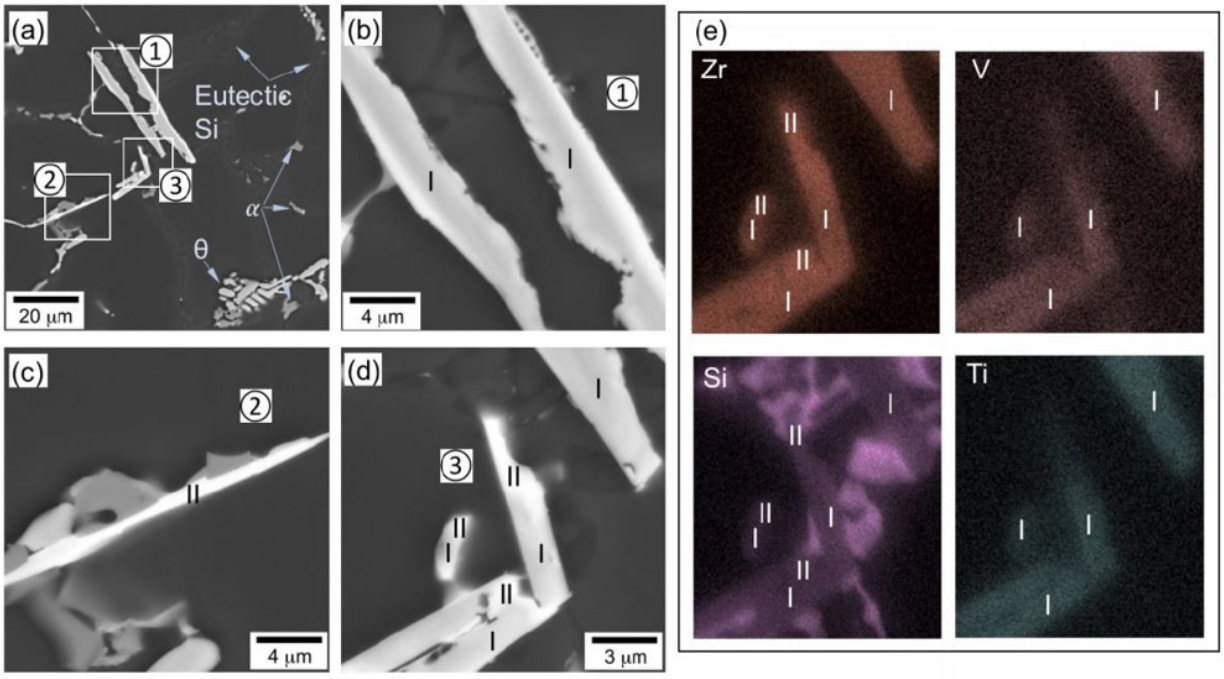

Figure 7.2.1: Graphical representation of (a) typical as-cast microstructure with multiple phases: FCC matrix, eutectic Si-phase, θ phase, α-Fe phase and two types of TM-containing primary phases; (b) Enlarged image of frame 1 in (a), showing the plate phase (Type I) with grey contrast; (c) Enlarged image of frame 2 in (a), showing the phase (Type II) with bright contrast; (d) Enlarged image of frame 3 in (a), showing the mixed phases of two types; (e) SEM-EDS maps of phases shown in (d), indicating that more V and Ti concentrated in Type I phase and Type II phase was enriched in Zr and traces of V and Ti.

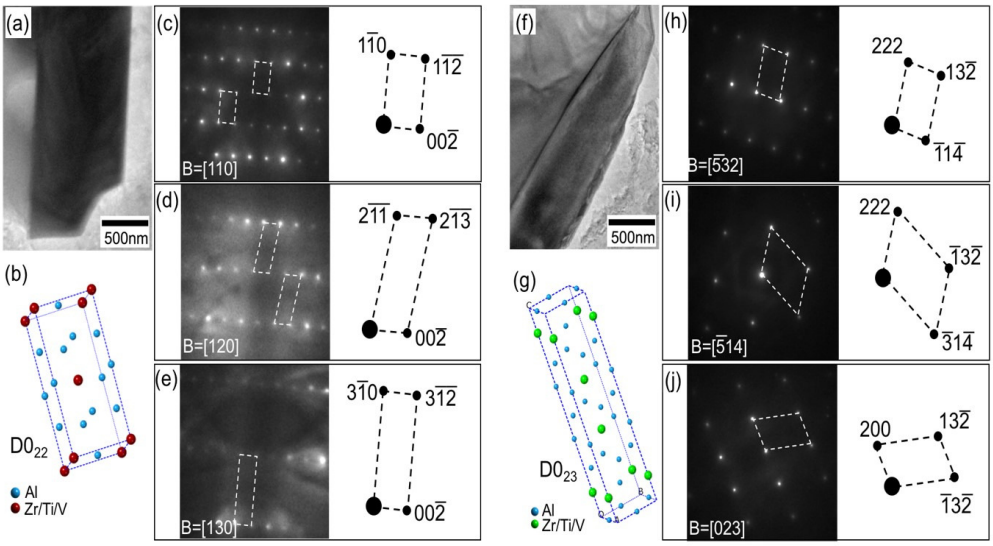

Figure 7.2.2: Graphical representation of TEM characterization and identification of primary TM-containing primary phases.

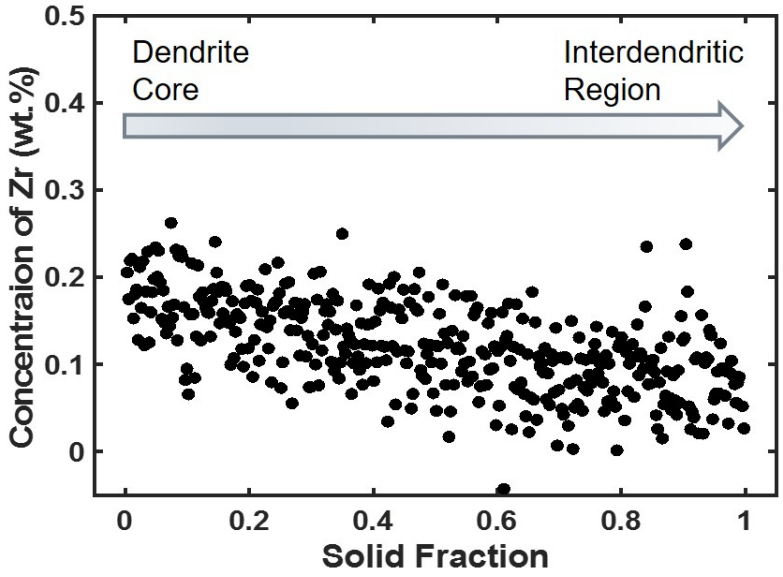

Figure 7.2.3: EPMA segregation profile of Zr as a function of the solid fraction

Then, after first stage aging, no change was observed in the bulky TM-containing primary phases. Nanometer scale precipitates containing TM elements formed in Al-matrix. Scanning transmission electron microscope (STEM) and APT were used to characterize the type, morphology, size and composition of these precipitates. As shown in the high angle annular dark field (HAADF) image in Figure 8(a), the precipitates appeared in a near-spherical shape with the size of ~4nm. The atomic structure of precipitates and their

interface with the Al-matrix were clearly captured by high resolution HAADF images taken from [100] and [110] zone axis (Figure 8(b)~ (e)). The crystal structure of L12 for the precipitates and the coherent interfacial relationship between them and Al-matrix were confirmed. Figure 8(f) gives the three-dimensional APT reconstruction on a Focused Ion Beam (FIB) lift-out tip made from the dendrite core. Only Zr atoms are shown here. The distribution of different elements in precipitates and Al-matrix was exhibited in the proxigram in Figure 8(g), which was produced after setting the position of a 3.75 at.% Zr as the isoconcentration surface for the precipitate 8 reconstructed. It could be seen that Zr and Si are two main concentrated elements in L12 precipitates. Based on the composition information from the proxigram, the formula of L12 phase in this alloy was proposed as (Al, Si, Mg)2.62(Zr, Ti, V, Cu).

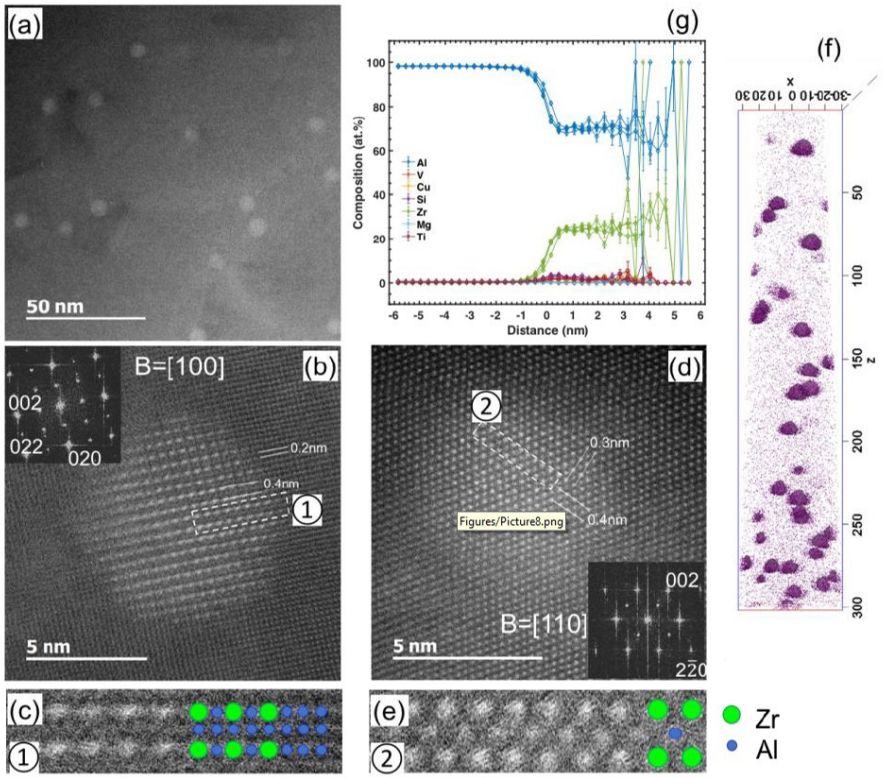

Figure 7.2.4 STEM and APT characterization on L12 precipitates with Zr. (a) HAADF-STEM image of precipitates; (b) HAADF-STEM image with high resolution of L12 phase taken from [100] zone axis; (c) Enlarge image of frame 1 in (b); (d) HAADF-STEM image with high resolution of L12 phase taken from [110] zone axis; (e) Enlarge image of frame 2 in (d); (f) Three-dimensional APT reconstructions. Only Zr atoms are shown here. (g) Proxigram displaying the distribution of different elements relative to the position of a 3.75 at.% Zr isoconcentration surface for the precipitate reconstructed.

Finally, a short duration solution treatment is used to avoid the coarsening of TM-containing precipitates formed in the first stage aging and ensure enough Cu/Mg to dissolve into Al-matrix. In the following second stage aging, a desired dual precipitation microstructure consisting of spherical TM-containing precipitates and plate shape Θ'-Al2Cu precipitates can be achieved, as shown in Figure 7.2.5. Such novel microstructure is thought to contribute the superior elevated temperature performance, as shown in previous section.

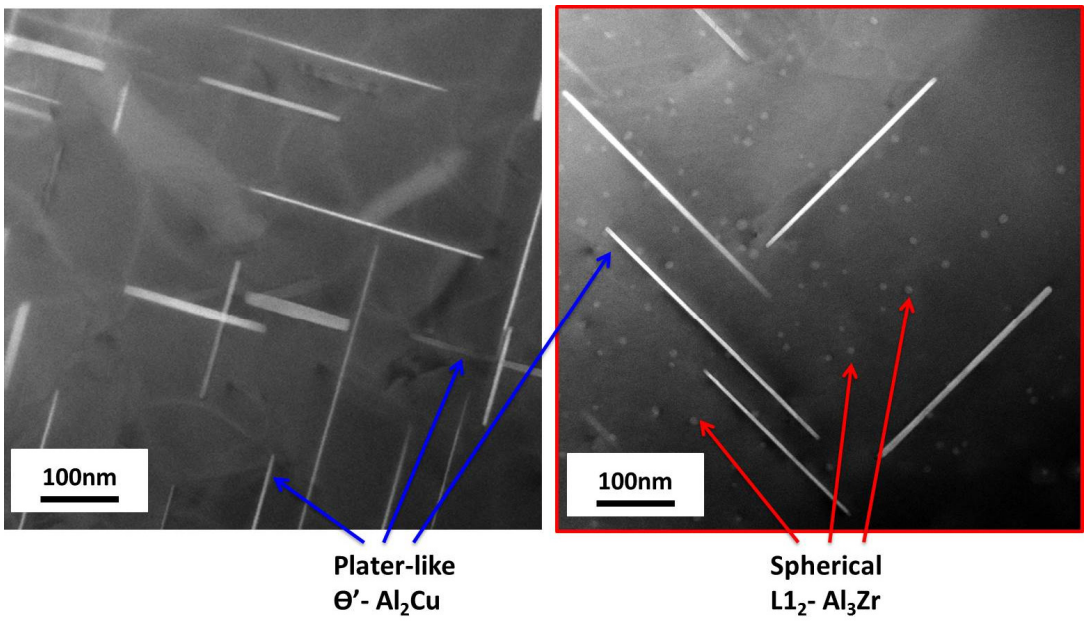

Figure 7.2.5 Graphical representation of dual precipitation microstructure observed in Ford-SPMC-3Stage

Task 3: Prototyping Demonstration

The prototyping demonstration for cylinder head alloys and engine block alloys has been finalized: For cylinder head alloys, Ford-SPMC-three-stage and AS7GU-T64 were made into 1.5L Dragon GTDI cylinder head at Qin'an China. For engine block alloys, ADC12Z-T5, Ford-HPDC-T5, and Alcoa's C677F-T5 were made at two different locations, Mag-tec at Michigan using a I4-Bearing-Beam die and Ryobi at Japan using a Journal Piece die.

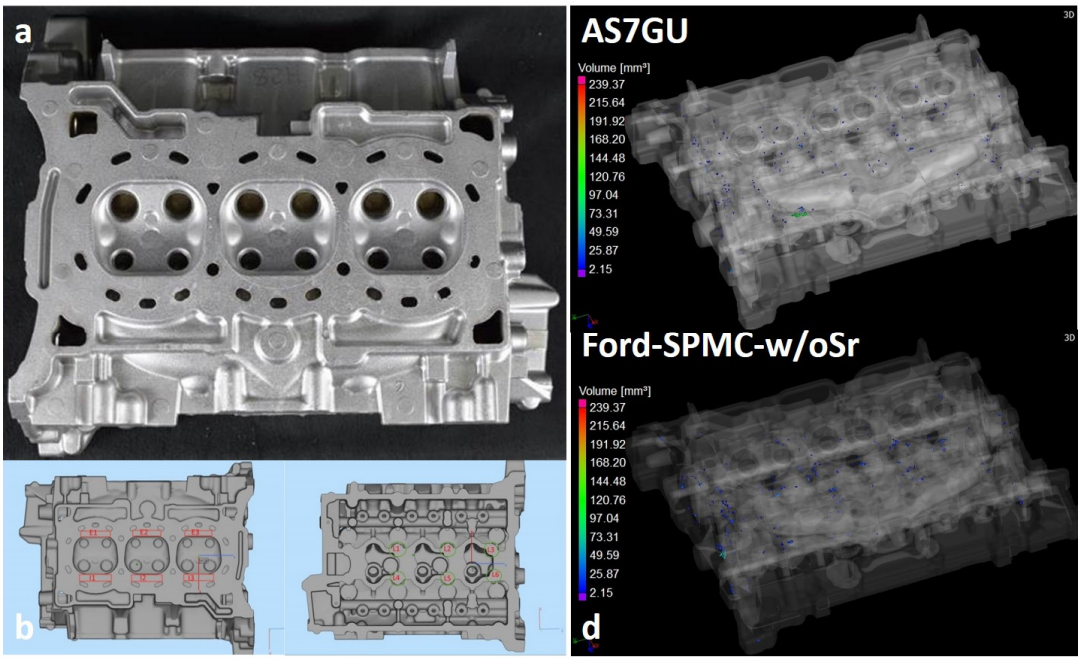

Figure 7.3.1: Graphical representation of (a) a 1.5L GTDI cylinder head prototyped with Ford-SPMC-w/oSr at Qin'an, China; (b) the locations from deck face (red rectangular) and bolt boss (green circle) for mechanical tests; (c) CT scan results for 1.5L GTDI cylinder heads showing the distribution of pores

First of all, 50 castings of GTDI cylinder head for three compositions, Ford-SPMC-w/Sr, Ford-SPMC-w/oSr and AS7GU, were made at Qin'an, China as shown in Figure 7.3.1. High quality castings are obtained, as indicated by CT scan shown in Figure 7.3.1(c). Samples used for tensile and endurance limit testing were sectioned from locations with different cooling rates in each GTDI cylinder head: bolt boss (Figure 7.3.1(b) right) with slow cooling rate and deck face (Figure 7.3.1(b) left) with fast cooling rate. After the sectioning, testing samples were heat-treated with corresponding conditions: novel three-stage heat treatment was used for Ford-SPMC-w/Sr and Ford-SPMC-w/oSr, and traditional T64 was used for AS7GU. In addition, 100 hours' pre-exposure at testing temperatures was performed after heat treatment. The samples, however, sectioned from GTDI heads are too small to be machined into the same geometry used by torpedo samples. As a result, the sub-size samples are used for both tensile and endurance limit test. The correlation between the sub-size and regular-size samples in mechanical properties was studied. According Figure 7.3.2 shown, both tensile properties and endurance limit for regular-size and sub-size samples machined from torpedo samples are comparable. Thus, geometries of testing samples have little impact on both tensile properties and endurance limit.

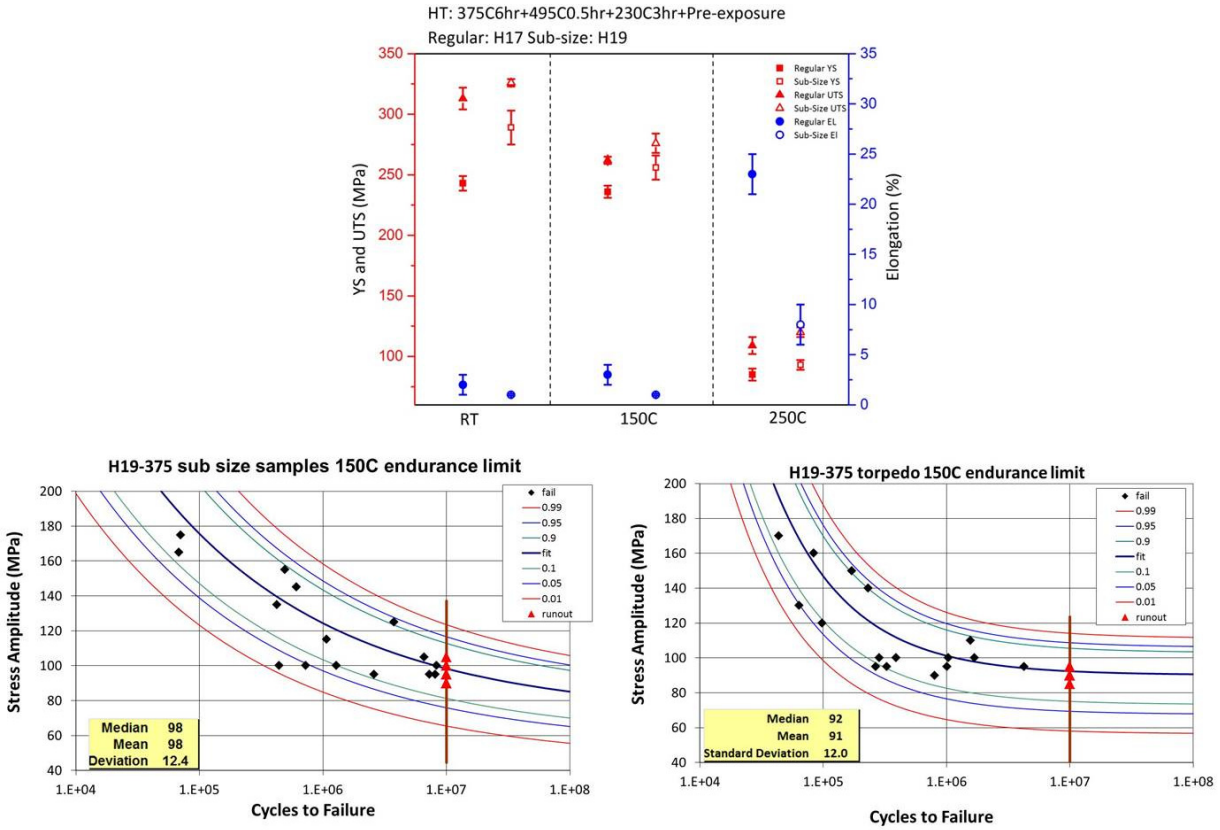

Figure 7.3.2: Graphical representation of tensile and endurance limit test results of sub-size and regular-size samples for torpedo Ford-SPMC, showing comparable mechanical properties

The tensile properties of AS7GU-T64, WSR-375 and WOSR-375 are summarized in Figure 7.3.3. Several conclusions can be draw from the tensile results. 1) YS and UTS decrease with increasing of testing temperatures, while the elongation increases with increasing of testing temperature. 2) YS and UTS have same behavior. The samples that have high YS also have high UTS. 3) YS and UTS of deck face are higher than bolt boss, and YS and UTS of blot boss are higher than torpedo samples. 4), YS and UTS of bolt boss for each composition are comparable to each other. 5) YS and UTS of deck for WSR-375 and WOSR-375 are higher than AS7GU-T64. 6) the elongation of torpedo samples is higher than deck face that is higher than bolt boss. 7) AS7Gu-T64 has higher elongation at low temperatures. 8)WSR has higher elongation than WOSR.

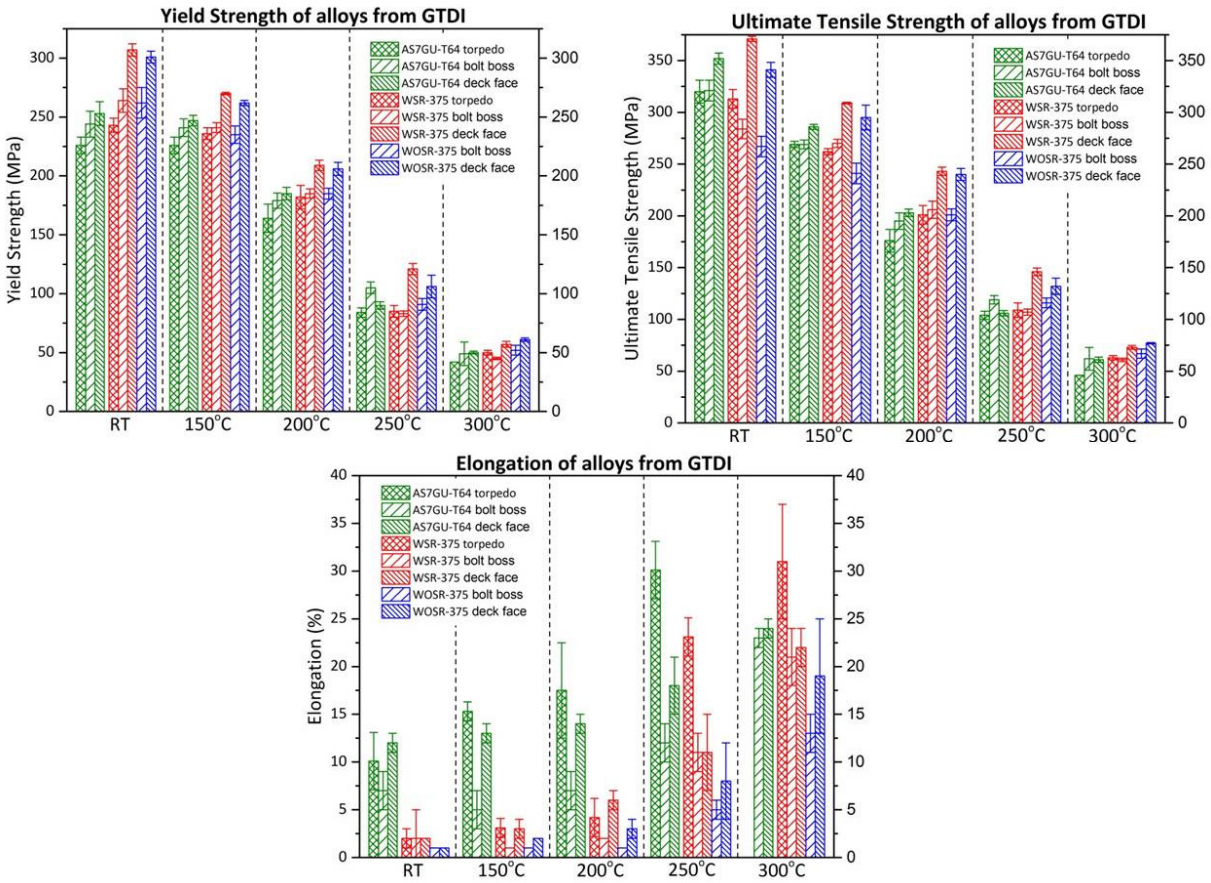

Figure 7.3.3: Graphical representation of tensile properties of AS7GU-T64, WSR-375 and WOSR-375

The results of endurance limit tests at elevated temperatures are shown in Table 7.3.2. Firstly, 150 ˚C high cycle fatigue (HCF) strength of deck face components from Ford-SPMC-w/Sr-375 and Ford-SPMC-w/oSr-375 is closed to that of torpedo samples, while 150 ˚C HCF strength of deck face components from AS7GU is much higher than that of torpedo samples. Then, the deck face components from AS7GU-T64 and Ford-SPMC-w/Sr-375 have comparable 150 ˚C HCF strength. When the testing temperature increases to 180 ˚C, the HCF strength of Ford-SPMC-w/Sr-375 is still above 90 MPa, while the HCF strength of AS7GU-T64 drops to 70 MPa. On the other hand, 150 ˚C HCF strength of bolt boss from AS7GU-T64 is above 70MPa, while Ford-SPMC-w/Sr-375 and Ford-SPMC-w/oSr-375 are below 60 MPa. It's well know that the pressure and temperature at deck face are much higher than that at bolt boss and most failures in cylinder heads happen at deck face. Thus, the improved elevated temperature endurance limit observed in Ford-SPMC-w/oSr-375 at deck face show promising to replace current used alloys for cylinder head application

Table 7.3.1 Elevated temperature HCF strength of torpedo samples, deck face and bolt boss from 1.5L GTDI cylinder heads, for AS7GU-T64, Ford-SPMC-w/Sr-3stage, and Ford-SPMC-w/oSr-3Stage

	Location	150 °C	180 °C
AS7GU-T64	Torpedo	62±6	
	Bolt boss	93±11	70±6
	Deck face	72±11	
Ford-SPMC-w/Sr-375	Torpedo	72±7	
	Bolt boss	67±7	
	Deck face	59±6	
Ford-SPMC-w/oSr-375	Torpedo	91±12	92±12
	Bolt boss	92±10	92±9
	Deck face	51±6	

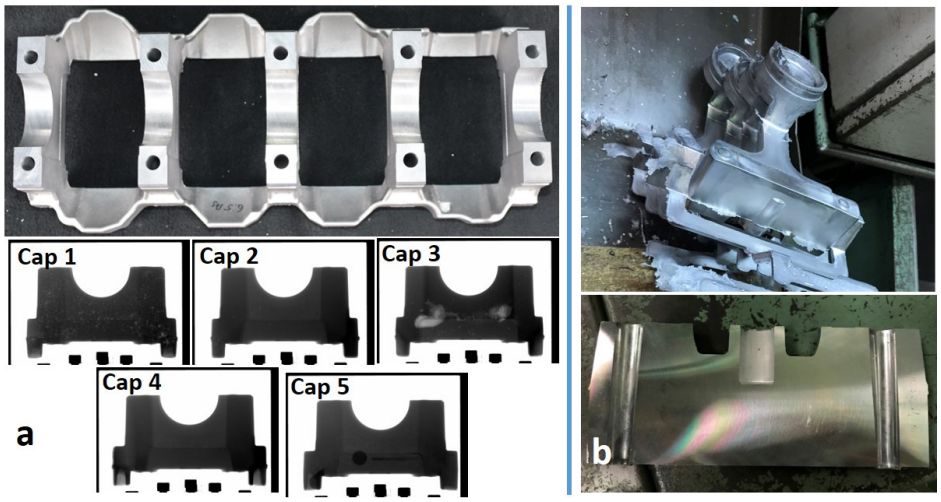

Figure7.3.4 Graphical representation of (a) a I4-Bearing-Beams castings prototyped with Ford-HPDC at Magtec, MI and X-ray results showing the distribution of pores; (b) a Journal-Piece castings prototyped with C677F at Ryobi, Japan and the cross-section showing no pores is observed

Two prototyping projects were conducted to test the performance of Ford-HPDC alloys under the process of high-pressure die cast. An I4-Bearing-Beam die with five caps was used at Magtec, MI, and a Journal-Piece die with only one cap was used at Ryobi, Japan. The HPDC machines and samples are shown in Figure 7.3.4. In addition, two other alloys are used as benchmark alloys: ADC12Z, current used alloys for engine block, and C677F, commercial alloys from Alcoa company. All the samples are heat-treated with conventional T5 condition with 100 hours' pre-exposure at testing temperatures for elevated temperature tests. The porosity of five caps from I4-Bearing-Beam is firstly examined by X-ray, as shown in Figure 7.3.4(a). Due to the relatively low porosity level comparing to other

caps, cap 4 is used for tensile and endurance limit tests. In addition, the cross section of Journal-Piece samples examined by optical microscope also shows low porosity. YS and UTS at three temperatures of torpedo, I4-Bearing Beam, and Journal-Piece samples are summarized in Figure 7.2.5(a) and (b), respectively. In general, torpedo samples for all three compositions, ADC12Z, Ford-HPDC, and C677F, have the highest YS and UTS from room temperature up to 300 ˚C, except for ADC12Z at room temperature. On the other hand, samples from I4-Bearing-Beam have the lowest tensile properties, although the locations with best quality are used for testing. The results of 150 ˚C endurance limit tests of these three castings show similar tendency as tensile tests: torpedo samples have the highest HCF strength, followed by Journal-Piece, and then I4-Bearing-Beam-Loc4. In fact, endurance limit tests were only performed for ADC12Z on I4-Bearing-Beam and its 150 ˚C HCF strength is just 36±4MPa. Lots of pores that is beyond the resolution of X-ray can be observed in the fracture surface from I4-Bearing-Beam by scanning electron microscope. It's shown that the high pressure die cast processes have limitation on casting samples with complicated geometries, like bearing beam and engine block. Instead of optimization of alloys' composition and heat-treatment, the processes, like gating, feeding, and so on, need to be further modified.

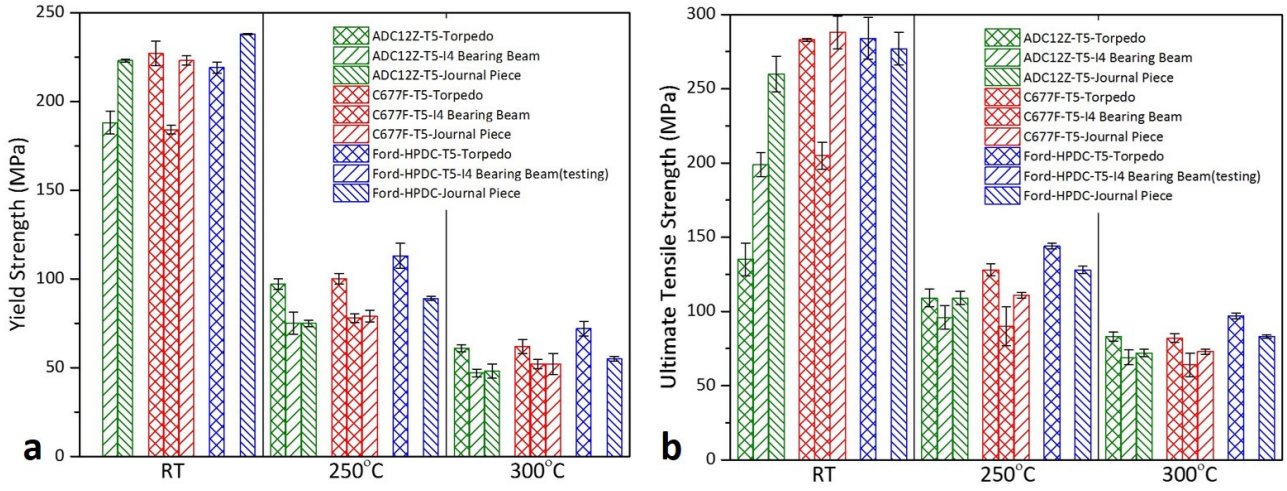

Figure 7.3.5 Graphical representation of (a) yield strength and (b) ultimate tensile strength at different temperatures of ADC12Z-T5, C677F-T5, and Ford-HPDC-T5 sectioned from torpedo, I4-Bearing-Beam, and Journal-Piece showing the mechanical properties of torpedo samples cannot be achieved by the process of high-pressure die cast

Task 4: The ICME Tools Development and Gap Identification

The microstructures of Ford-SPMC at different heat treatment stages, including as-cast, first-stage aging, solution treatment, and second-stage aging are studied by different ICME tools and the gaps between simulation and experiments are identified.

Scheil solidification model is used to simulate the solidification pathway of Ford-SPMC alloys, which is available in both ThermoCalc and Pandat. The Scheil simulation indicates that the solidification pathway is Zr/V-containing primary precipitates → fcc-Al matrix → Al-Si eutectic → beta-Al9Fe2Si2 → theta-Al2Cu → Q-AlMgSiCu. This result shows well agreement with SEM observation, as Figure 7.4.1 shown. The quantitative results from Scheil model, however, show inconsistent with DSC result. First, the transformation temperatures in Scheil model are off from DSC measurement. Then, the fractions of phases predicted by Scheil model are not related to solidification rates. But, DSC measurement shows that the fractions of phases, especially Theta-Al2Cu phase, change with solidification. A robust model, which takes solidification rates into account, is on-demand.

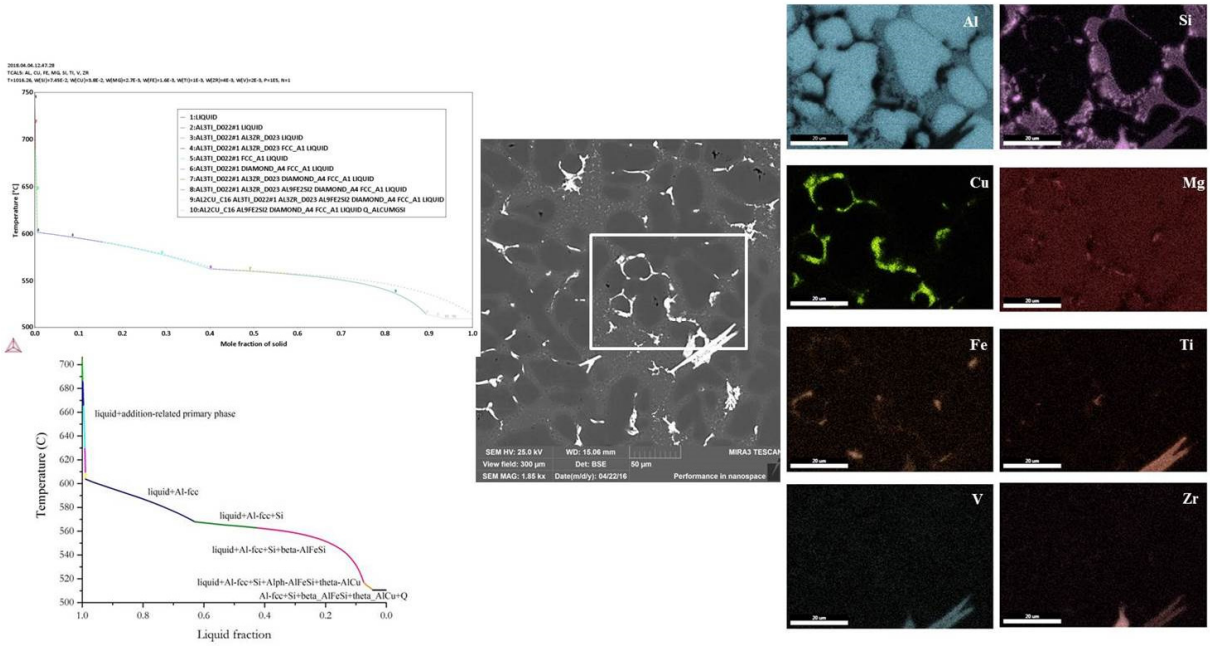

Figure 7.4.1: Graphical representation of Scheil solidification simulation of Ford-SPMC alloys showing well agreement with SEM observation

First-stage aging to form spherical shape Zr-containing precipitates is simulated by two different ICME tools, using Kampmann and Wagner numerical method: TC-PRISMA with TCAL5 and MOBAl3 database, PanPrecipitation with PanAl-TH+MO-2017 database. Experimental data, such as precipitates size and number density of Zr-containing precipitates, are obtained from TEM and SAXS. Through optimization of kinetic database, the simulation results show good agreement with experimental results, as Figure 7.4.2 shown.

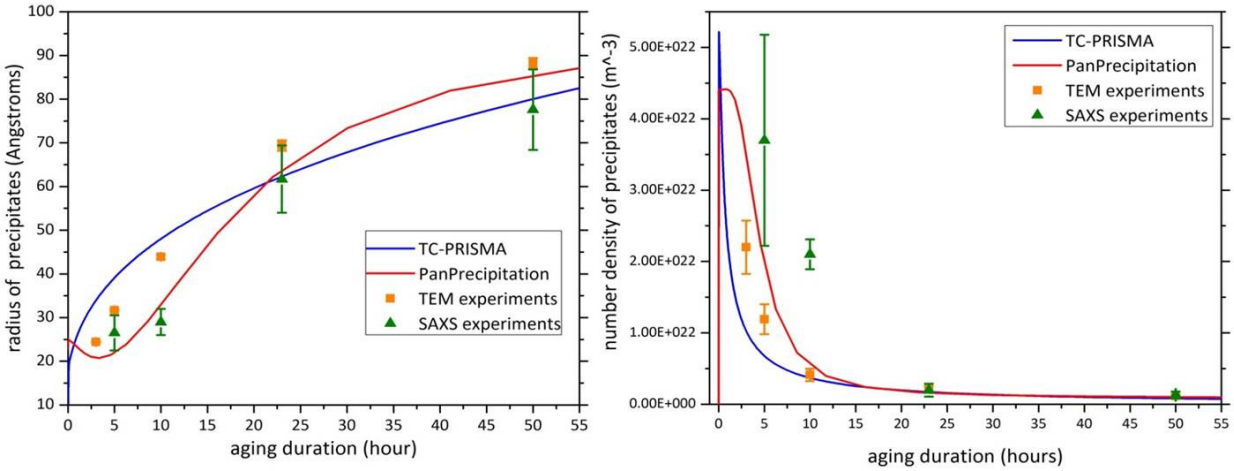

Figure 7.4.2: Graphical representation of precipitation simulation of Ford-SPMC alloys during first stage-aging suing TC-PRISMA and PanPrecipitation

Solution treatment at 495 ˚C to dissolve Cu-containing phases for Ford-SPMC and AA319 is simulated by DICTRA developed by ThermoCalc. The simulated results are compared with DSC results. Both Ford-SPMC and AA319 are solutionized at 495 ˚C for different duration, followed by quenched. The heating DSC curves of Ford-SPMC and AA319 with different solution treatment time are shown in Figure 7.4.3. The last two peaks in DSC curves are related to the melting of Cu-containing phases left in samples. It's clearly shown that and their fractions decrease with increasing of solution treatment time. Due to the lack of some important information, such as the latent heat and formula of phase transformation, the fraction of Cu-containing phases cannot be obtained directly from DSC results. A reduced fraction is proposed here, which is the ration of Cu-containing phases in samples after solution treatment to that in as-cast sample. Based on two assumptions: 1) solution treatment only dissolves Cu-containing phases, but doesn't affect other phases; 2) formula of melting of Cu-containing phases are fixed, the reduced fraction can be expressed as

$$\frac{f_{n=0.5,1,2,4,8}}{f_{n=0}} = \frac{1-Area_{n=0.5,1,2,4,8}^{theta/Q}}{1-Area_{n=0}^{theta/Q}} \times \frac{Area_{n=0}^{theta/Q}}{Area_{n=0.5,1,2,4,8}^{theta/Q}}.$$

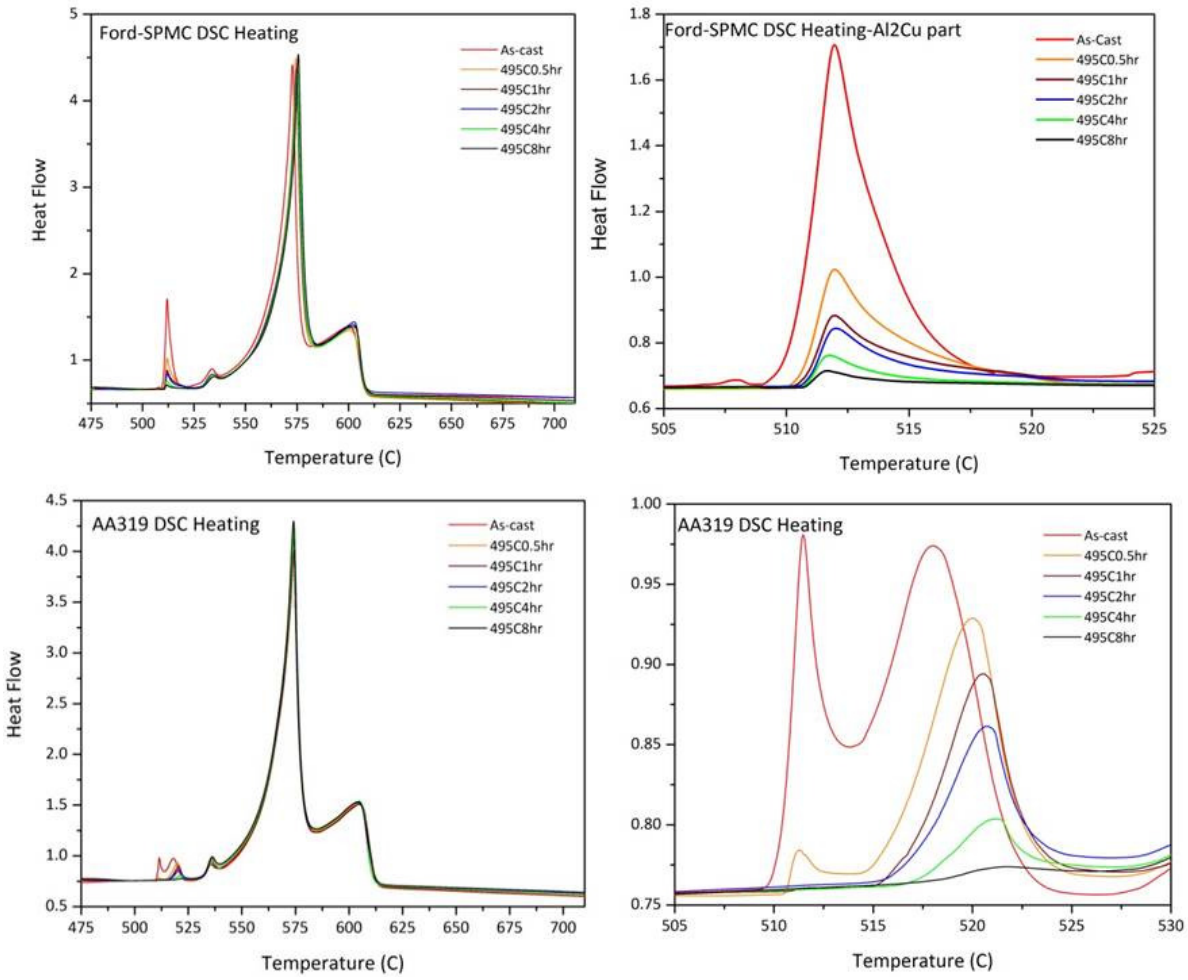

Figure 7.4.3: Graphical representation of heating DSC result of Ford-SPMC and AA319 with different solution treatment time, showing Cu-containing phases dissolve during heat treatment

Simulation of solution treatment is performed in DICTRA using TCAL5 thermodynamic database and MOBAl3 mobility database. Four geometries are considered: planer, cylinder, sphere-1, and sphere-2, as figure 7.4.4 shown. The reason results are obtained in planer and sphere-2. The initial conditions, the fraction of Cu-containing phases, are obtained from Schiel prediction and density data in literature. With modification of diffusivity, simulated results show good agreement with experiment results, as figure 7.4.5 shown. The gaps, however, still exist: 1) Zr and V can be included, 2) more reasonable geometry is needed.

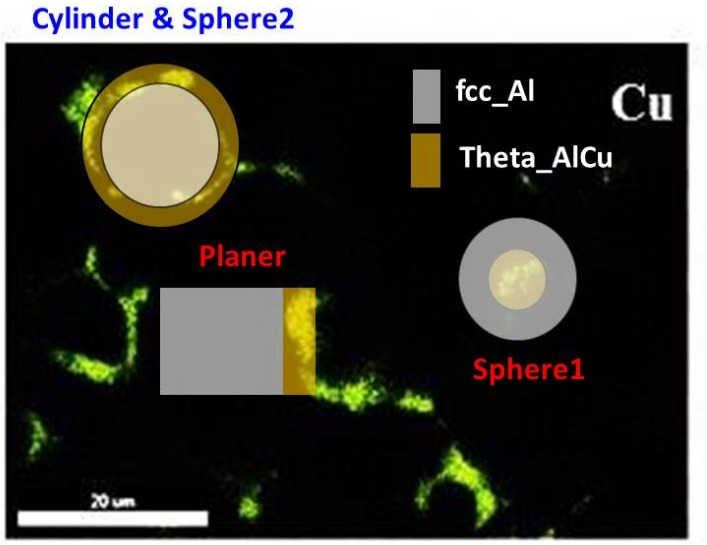

Figure 7.4.4: Graphical representation of four geometries used in DICTRA simulation

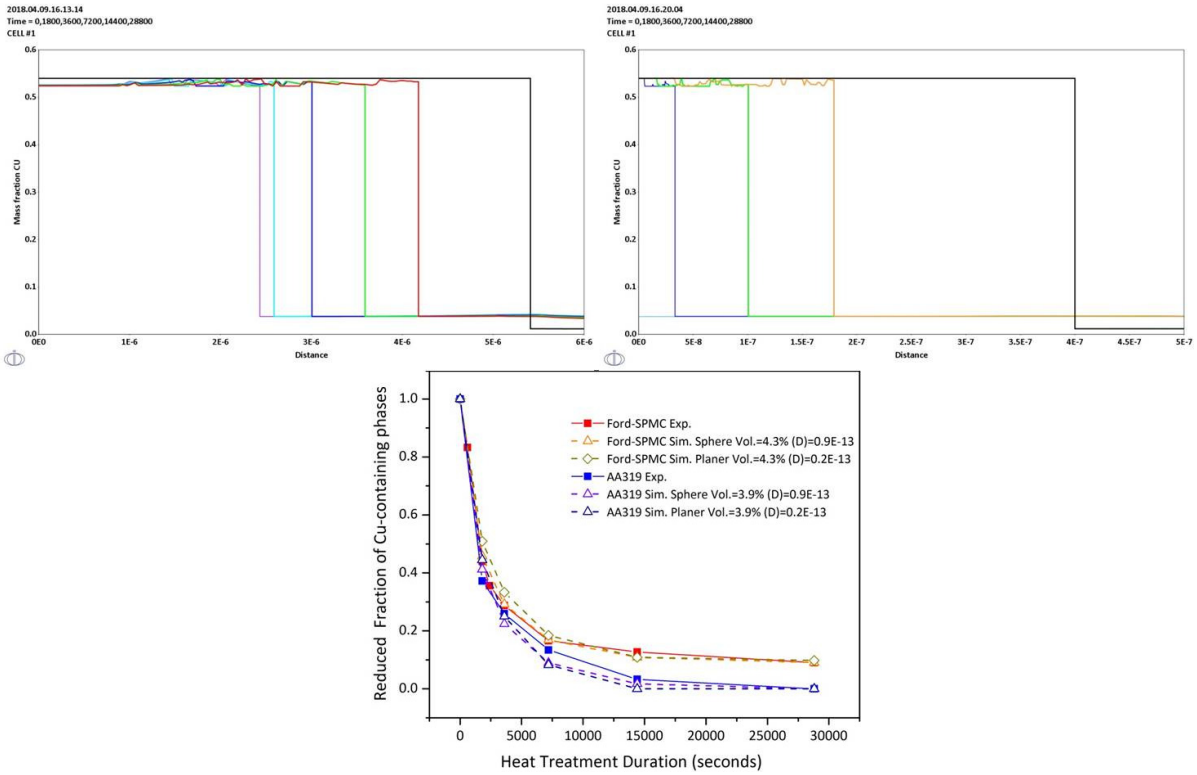

Figure 7.4.5: Graphical representation of DICTRA simulation of solution treatment of Ford-SPMC and AA319, comparing with DSC results

Second stage aging to form plate-like Al2Cu precipitates are also simulated by KWN model. KWN model is a one-dimension model and can only simulate the spherical shape precipitates. As a results, an equivalent sphere will be assumed for plate shape precipitates:

$$r_{eq} = \sqrt[3]{\frac{3}{4} dia^2 * thickness}$$

The precipitation kinetics of Al2Cu precipitates in AA319 alloys at several temperatures were characterized and published by Ford (S.C. Weakly-Bollin, W. Donlon, C. Wolverton, J.W. Jones and J. E. Allison, Metallurgical and Materials Transaction 35A, 2408(2004)). The PanPrecipitation simulated results, comparing with experimental data, are shown in Figure 7.4.6. It's shown that the KWN model doesn't work well for plate-shape precipitates. The phase field model is better choice for plate-shape precipitates.

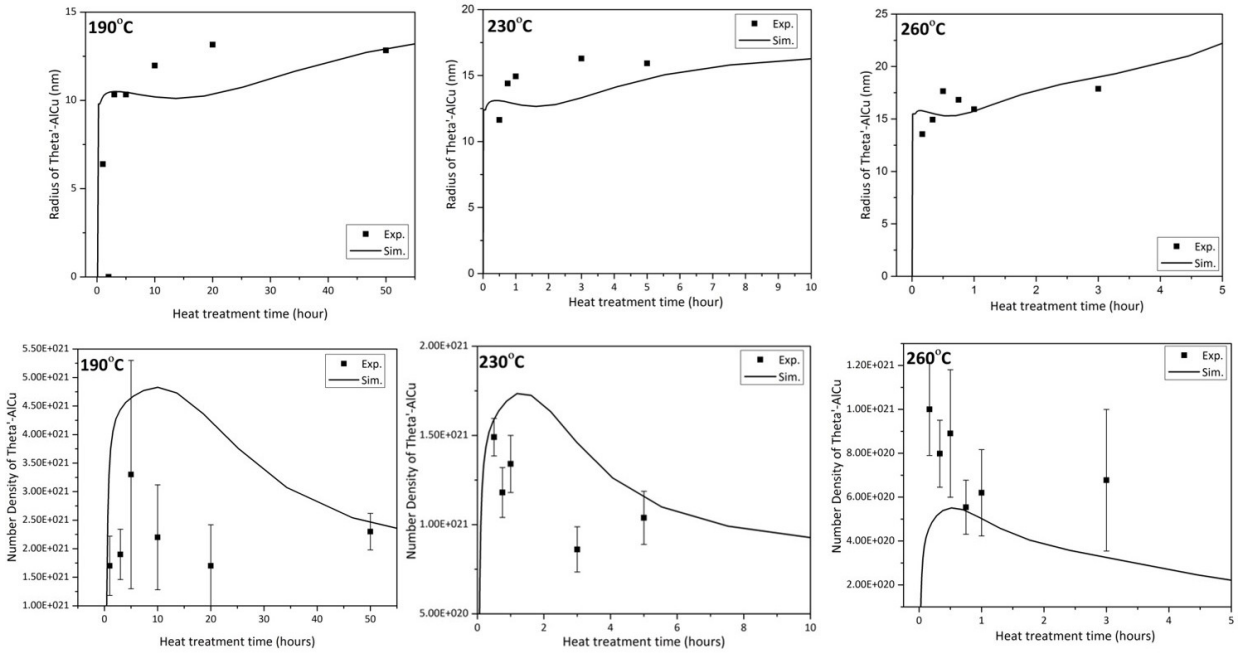

Figure 7.4.6: Graphical representation of Panprecipitation simulation of precipitation kinetics of Al2Cu plate-shape precipitates in AA319 alloys at different temperature.

Task 5: The Development of Cost Model

A cost model covering all the processes in sand casting, such as molding, melting, casting, heat-treatment, is used to estimate the premium of new alloys, as Figure 7.5.1 shown. First of

all, the GTDI cylinder head mold is used, where the geometric of the semi-permanent die and weight of castings are adjusted according to GTDI mold. Secondly, prices for baseline alloy (AS7GU) and new alloys with transition metal additions are inquired from suppliers. Thirdly the power input to melt Ford-SPMC alloys is increased, since the melting temperatures of Ford-SPMC alloys are higher than baseline alloys. At last, a novel three-stage heat treatment is used for Ford-SPMC alloys. This three-stage heat treatment needs more labor cost because there are three steps rather than two steps in T7 and T64. But the power input of this heat treatment is lower, since the high temperature solution treatment is shorter. The results are shown in Figure 7.5.2. It's indicated that the total premium of Ford-SPMC-three stage is 11.8% over the AS7GU-T64, which is closed to the DOE target, 10%. The melting&casting and heat treatment mainly contribute to the premium.

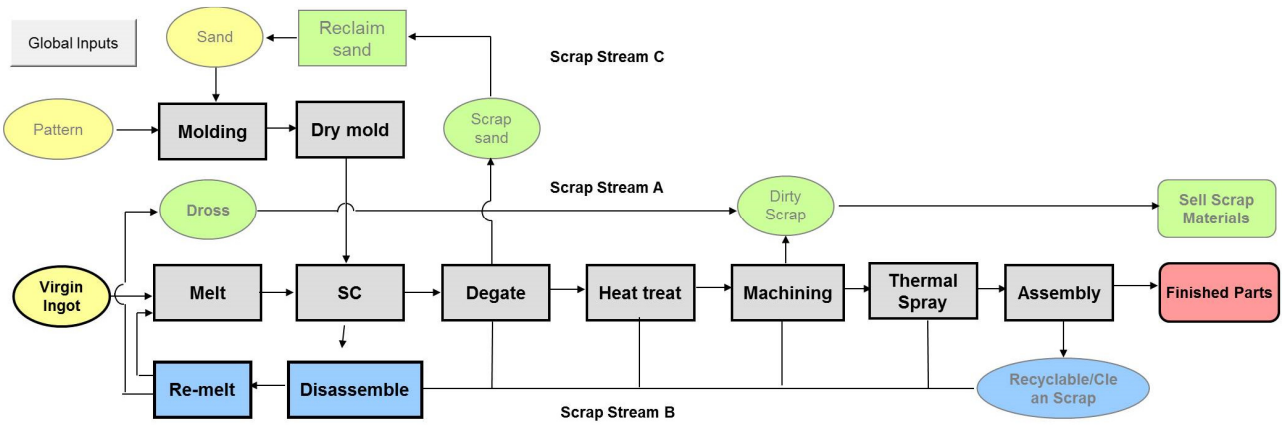

Figure 7.5.1: Graphical representation sand cost model

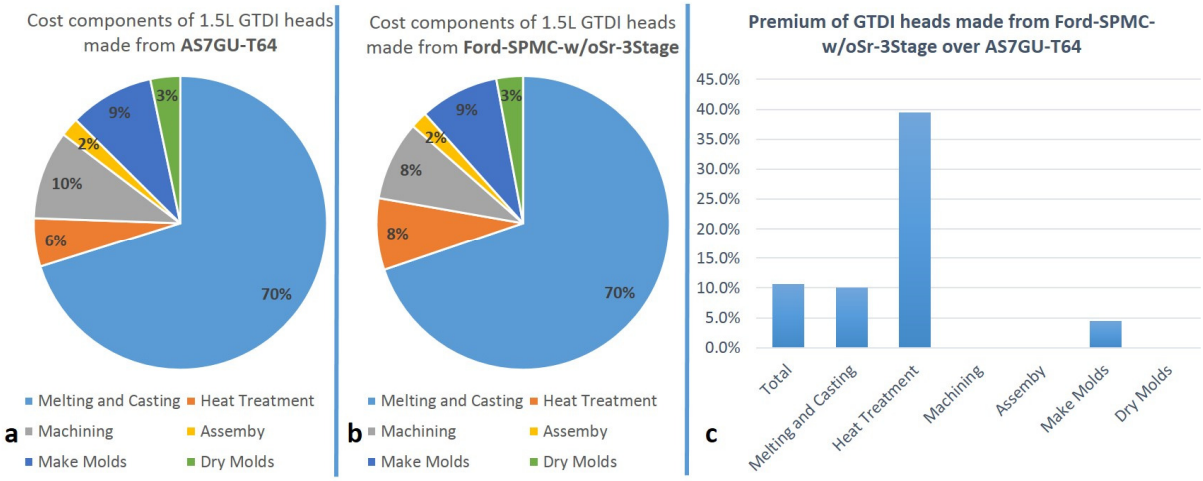

Figure 7.5.2: Graphical representation of the cost components calculated by the cost model of 1.5L GTDI head made from (a) AS7GU-T65 and (b) Ford-SPMC-w/oSr-3stage; (c) the premium of GTDI heads made from Ford-SPMC-3stage over AS7GU-T64 showing the new alloys do not exceed 110% of the cost using incumbent alloys

8. Remarks

Two aluminum alloys, Ford Semi-Permanent Mold Cast with novel three-stage heat treatment and Ford High-Pressure Die Cast with T5 heat treatment, are developed with the guidance of ICME method in this project, which are applicable for cylinder head and engine block application, respectively. Five remarks are shown as following:

a) The torpedo samples prepared at Ford laboratory for Ford-SPMC-3stage and Ford-HPDC-T5. Through extensive mechanical tests, it has been shown that these two alloys have superior properties over baseline alloys and can meet all the requirements proposed by DOE. Especially, the elevated temperature HCF strength of Ford-SPMC-three-stage and Ford-HPDC-T5 is above 90 MPa, which is much higher than the currently used alloys, AS7GU, for high performance engines. To the knowledge of the authors, these two alloys have the best HCF performance at elevated temperatures (>150 °C) in all the aluminum alloys intend for engine application;

b) Several advanced electron microscopes, including SEM, TEM, EPMA, APT, and so on, are employed to understand the mechanisms resulting in the superior elevated temperature performance of Ford-SPMC-3stage and Ford-HPDC-T5. For Ford-SPMC-3stage, a novel dual precipitation microstructure consisting of spherical TM-containing precipitates and plate shape Θ'-Al2Cu precipitates is achieved. And the coarsening resistance of Θ'-Al2Cu precipitates to elevated temperatures is well improved in Ford-

HPDC-T5. Such microstructures contribute to the superior elevated temperatures for these two alloys;

c) The performance of Ford-SPMC-3stage and Ford-HPDC-T5 are demonstrated on component level through several prototyping plans: 1) through 1.5L GTDI cylinder head project, it's demonstrated that Ford-SPMC-3stage has great high-temperature performance in deck face and both tensile and endurance can achieve the properties from torpedo samples, and 2) the performance of Ford-HPDC-T5 is limited by the process of high-pressure die cast and the properties cannot achieve that from torpedo samples. The component level demonstration provides us opportunities to collaborate internally to redesign engines with higher performance by less weight;
d) Several existing ICME tools, mainly including ThermoCalc, Pandat, and MagmaSoft, are evaluated and used in this project to provide guidance in alloys and heat-treatments design, and casting process optimization. Although some gaps between simulation and experiment still exist, the whole processes, from initial alloys design to component level demonstration, are significantly shorten to 5 years, and lots of cost saving opportunities are realized;
e) According to the comprehensive cost model develop internally, the total premium for a 1.5L GTDI heads from Ford-SPMC-3stage is 10.5% over the AS7GU-T64. This is within the DOE target that the components manufactured with these new alloys do not exceed 110% of the cost using incumbent alloys.

9. Cost Status:

QTR	From	To	Estimated Federal Share of Outlays	Actual Federal Share of Outlays	Estimated Recipient Share of Outlays	Actual Recipient Share of Outlays	Cumulative Estimated	Cumulative Actual
BP1- 02/01/13 - 01/31/14								
1Q13	1/1/2013	3/30/2013	238,846	15,704	102,363	6,731	341,209	22,435
2Q13	4/1/2013	6/30/2013	238,846	28,498	102,363	12,213	682,417	63,146
3Q13	7/1/2013	9/30/2013	238,846	56,232	102,363	24,099	1,023,626	143,477
4Q13	10/1/2013	12/31/2013	238,846	37,750	102,362	16,179	1,364,834	197,406
BP2- 02/01/14 - 01/31/15								
1Q14	1/1/2014	3/30/2014	270,957	63,226	116,124	27,097	1,751,915	287,728
2Q14	4/1/2014	6/30/2014	270,957	157,444	116,124	67,476	2,138,996	512,649
3Q14	7/1/2014	9/30/2014	270,957	126,344	116,124	54,148	2,526,077	693,141
4Q14	10/1/2014	12/31/2014	270,957	236,446	116,124	101,334	2,913,158	1,030,921
BP3-02/01/15-11/30/17								
1Q15	1/1/2015	3/30/2015	150,402	209,037	64,458	89,587	3,128,018	1,329,544
2Q15	4/1/2015	6/30/2015	150,402	149,382	64,458	64,021	3,342,878	1,542,947
3Q15	7/1/2015	9/30/2015	150,402	287,996	64,458	123,427	3,557,738	1,954,370
4Q15	10/1/2015	12/31/2015	150,402	212,798	64,458	91,199	3,772,598	2,258,367
No Cost Extension - 11/30/16								
1Q16	1/1/2016	3/30/2016	75,201	264,569	32,229	113,387	3,880,027	2,636,324
2Q16	4/1/2016	6/30/2016	75,201	232,520	32,229	99,652	3,987,456	2,968,496
3Q16	7/1/2016	9/30/2016	75,201	144,225	32,229	61,811	4,094,886	3,174,532
4Q16	10/1/2016	12/31/2016	75,201	163,471	32,229	70,059	4,202,315	3,408,062
No Cost Extension - 08/31/18								
1Q17	1/1/2017	3/30/2017	75,201	249,713	32,229	107,020	4,309,745	3,764,795
2Q17	4/1/2017	6/30/2017	75,201	194,453	32,229	83,337	4,417,174	4,042,585
3Q17	7/1/2017	9/30/2017	75,201	239,966	32,229	102,843	4,524,603	4,385,394
4Q17	10/1/2017	12/31/2017	75,201	172,647	32,229	73,992	4,632,033	4,632,033
1Q18	1/1/2018	3/30/2018	-	-	-	-	-	-
2Q18	4/1/2018	6/30/2018	-	-	-	-	-	-
3Q18	7/1/2018	8/31/2018	-	-	-	-	-	-
		Program Total	**3,242,423**	**3,242,423**	**1,389,610**	**1,389,610**	**4,632,033**	**4,632,033**

General Note: DOE Laboratory partner spending should not be included in the above table.

General Note: The information in this table should be consistent with the information provided in section 10 of the quarterly financial status reports (SF269 or SF269A).

10. Patents / Patent Applications:

Patent application, "Advanced Cast Aluminum Alloys for Automotive Engine Application with Superior High-Temperature Properties," filed on July 28, 2017.

11. Publications/Presentations:

Shi, Q., Huo, Y., Berman, T., Ghaffari, B., Li, M., Allison, J., Distribution of transition metal elements (Zr, V, Ti) in a 319-type aluminum alloy, submitted to Scripta Materialia